ISSN 1674-1056
http://cpb.iphy.ac.cn
http://iopscience.iop.org/cpb
中国物理 B
Chinese Physics
中国物理 Chinese Physics B

Analysis of resonance asymmetry phenomenon in resonator integrated optic gyro

Yao Fei(费瑶), Yu-Ming He(何玉铭), Xiao-Dong Wang(王晓东), Fu-Hua Yang(杨富华), Zhao-Feng Li(李兆峰)

Citation: Chin. Phys. B . 2018, 27(8): 084213. **doi:** 10.1088/1674-1056/27/8/084213

Journal homepage: http://cpb.iphy.ac.cn; http://iopscience.iop.org/cpb

What follows is a list of articles you may be interested in

Guiding properties of proton-implanted Nd^{3+}-doped phosphate glass waveguides

Qi-Feng Zhu(朱其峰), Yue Wang(王玥), Jian-Ping Shen(沈建平), Hai-Tao Guo(郭海涛), Chun-Xiao Liu(刘春晓)

Chin. Phys. B . 2018, 27(5): 054218. **doi:** 10.1088/1674-1056/27/5/054218

Plasmonically induced reflection in metal-insulator-metal waveguides with two silver baffles coupled square ring resonator

Zhi-Dong Zhang(张志东), Lian-Jun Ma(马连俊), Fei Gao(高飞), Yan-Jun Zhang(张彦军), Jun Tang(唐军), Hui-Liang Cao(曹慧亮), Bin-Zhen Zhang(张斌珍), Ji-Cheng Wang(王继成), Shu-Bin Yan(闫树斌), Chen-Yang Xue(薛晨阳)

Chin. Phys. B . 2017, 26(12): 124212. **doi:** 10.1088/1674-1056/26/12/124212

All polymer asymmetric Mach-Zehnder interferometer waveguide sensor by imprinting bonding and laser polishing

Yu Liu(刘豫), Yue Sun(孙月), Yun-Ji Yi(衣云骥), Liang Tian(田亮), Yue Cao(曹悦), Chang-Ming Chen(陈长鸣), Xiao-Qiang Sun(孙小强), Da-Ming Zhang(张大明)

Chin. Phys. B . 2017, 26(12): 124215. **doi:** 10.1088/1674-1056/26/12/124215

Angular-modulated spatial distribution of ultrahigh-order modes assisted by random scattering

Xue-Fen Kan(阚雪芬), Cheng Yin(殷澄), Tian Xu(许田), Fan Chen(陈凡), Jian Li(李建), Qing-Bang Han(韩庆邦), Xian-Feng Chen(陈险峰)

Chin. Phys. B . 2017, 26(11): 114210. **doi:** 10.1088/1674-1056/26/11/114210

Tunable optical filter using second-order micro-ring resonator

Lin Deng(邓林), Dezhao Li(李德钊), Zilong Liu(刘子龙), Yinghao Meng(孟英昊), Xiaonan Guo(郭小男), Yonghui Tian(田永辉)

Chin. Phys. B . 2017, 26(2): 024209. **doi:** 10.1088/1674-1056/26/2/024209

Analysis of resonance asymmetry phenomenon in resonator integrated optic gyro*

Yao Fei(费瑶)[1,2], Yu-Ming He(何玉铭)[1,2], Xiao-Dong Wang(王晓东)[1,3], Fu-Hua Yang(杨富华)[1,3], and Zhao-Feng Li(李兆峰)[1,3,†]

[1] *Engineering Research Center for Semiconductor Integrated Technology, Institute of Semiconductors, Chinese Academy of Sciences, Beijing* 100083, *China*

[2] *College of Materials Science and Opto-Electronic Technology, University of Chinese Academy of Science, Beijing* 100049, *China*

[3] *School of Microelectronics, University of Chinese Academy of Sciences, Beijing* 100049, *China*

(Received 18 October 2017; revised manuscript received 12 March 2018; published online 10 July 2018)

Resonator integrated optic gyro (RIOG) is a high-accuracy gyroscope based on the Sagnac effect. The waveguide-type ring resonator is a key rotation sensing element in the RIOG. An asymmetric resonance line shape is found in the optic resonator. These asymmetries will induce offset errors when the phase modulation spectroscopy technique (PMST) is applied to the RIOG. The polarization errors and the difference among normal mode losses are found to be the two main sources of resonance asymmetry in an experiment. These sources are fully investigated and their contributions to the offset errors are compared. The analysis shows that proper modulation frequencies in clockwise (CW) and counterclockwise (CCW) directions can reduce an RIOG bias error. A transmissive resonator is recommended to obtain a better resonance line shape.

Keywords: gyroscopes, optical sensing and sensors, resonators

PACS: 42.79.Gn, 42.81.Pa, 42.82.–m **DOI:** 10.1088/1674-1056/27/8/084213

1. Introduction

An optical gyroscope is a high-accuracy inertial rotation sensor based on the Sagnac effect.[1] Compared with an interferometer optic gyro (IOG), a resonator optic gyro (ROG) can achieve the same performance as an IOG which is two orders of magnitude longer in optical length than that of ROG,[2] and hence the ROG has the potential to achieve advantages of high accuracy, small size, and low cost. A resonator integrated optic gyro (RIOG) is a waveguide-type ROG. To improve the short-noise limited sensitivity,[3] the waveguide-type ring resonator (WRR) is suggested to be low-loss and high-finesse. Equipped with a high-finesse waveguide-type ring resonator, RIOG has achieved a bias stability of $0.004^\circ/\mathrm{s}$ over a one-hour timeframe.[4] However, the RIOG still cannot meet the requirements of applications in defense and aerospace where a bias drift $\leq 1^\circ/\mathrm{h}$ and a resolution $\leq 10^\circ/\mathrm{h}$ are required.[5]

Resonance asymmetry of the WRR is another feature that affects an RIOG performance.[6] In the RIOG, the readout system is based on the phase modulation spectroscopy technique (PMST).[7] Different modulation frequencies are applied to the clockwise (CW) and counterclockwise (CCW) beams to reduce the backscattering induced noise.[8] When the resonance line-shape is asymmetric in the WRR, a bias error will be introduced into the gyro's output.[6] Based on the results from the experiments, two sources of resonance asymmetry are analyzed. The two sources are polarization errors[9] and different normal mode losses in the coupler.[10] Resonance asymmetry degree (RAR) is used to evaluate the asymmetric degree of the resonance curve.[11]

In this paper, the main parameters that affect the RAR in these sources are discussed in detail. Examining the influence of the RAR on bias error numerically, it is found that the gyro's bias error is proportional to the RAR of the resonance line shape. To reduce the bias error, a transmissive resonator is recommended to obtain a better resonance line shape. It is proved that proper modulation frequencies in CW and CCW directions can reduce an RIOG bias error.

2. System configuration

Figure 1 shows the experimental setup of the RIOG with a reflector WRR based on PMST. Points A and B are two contact points between fiber and WRR after being packaged. The couplers C1, C2, C3 are all 3-dB couplers. The output light from an FL is equally divided by coupler C1. The PM1 and PM2 are driven by the sinusoidal waveforms from internal reference signals of LIA1 and LIA2 with the frequencies f_1 and f_2, respectively. The CW and CCW beams in the WRR are sensed by photodetectors PD1 and PD2, respectively. Then, the CW and CCW signal are demodulated by LIA1 and LIA2, respectively. The demodulation signal from the CW signal is

*Project supported by the National Key Research and Development Program of China (Grant No. 2016YFA02005003) and the National Natural Science Foundation of China (Grant Nos. 61274066, 61504138, and 61474115).

†Corresponding author. E-mail: lizhaofeng@semi.ac.cn

© 2018 Chinese Physical Society and IOP Publishing Ltd

used to lock the center frequency of the fiber laser at the resonance frequency through PI. The signal from LIA2 is used as the gyro output, which is proportional to the resonant frequency difference between the CW signal and the CCW signal. The rotation rate is obtained from the frequency difference according to the Sagnac effect[1]

$$\Delta f = \frac{4A}{\lambda nL}\Omega, \tag{1}$$

where A is the area of the WRR, λ is the wavelength of fiber laser, n is the index of refraction, L is the length of WRR, and Ω is the rotation rate.

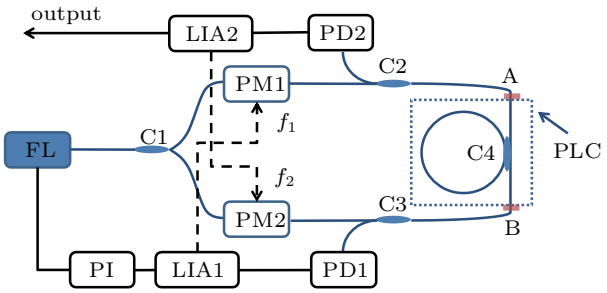


Fig. 1. (color online) System configuration of RIOG based on PMST. FL: fiber laser; C1, C2, C3, C4: couplers; PM1, PM2: phase modulators; PLC: planar lightwave circuit; PD1, PD2: photodetectors; LIA1, LIA2: lock-in amplifiers; PI: proportional integrator.

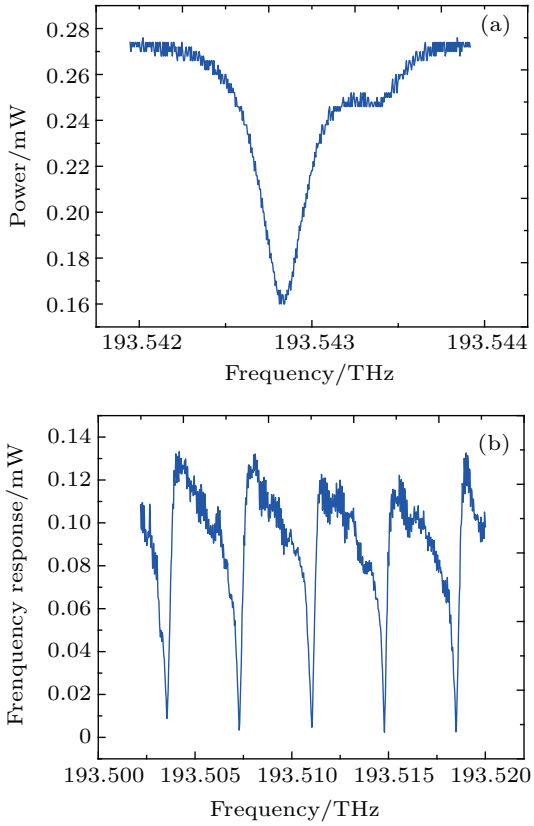


Fig. 2. (color online) Measured resonance curve of the lightwaves in (a) silica WRR, and (b) silicon nitride WRR.

Figures 2(a) and 2(b) show two types of resonance asymmetry phenomena observed in the experiments from a silica WRR and a silicon nitride WRR, respectively. The cross sections of the waveguide core of the silica WRR and silicon nitride WRR are shown in Figs. 3(a) and 3(b), respectively. The coupling coefficients of the silica WRR and the silicon nitride WRR are designed to be 0.15 and 0.12, respectively. Both of the two WRRs are of reflector-type. The lengths of the silica WRR and the silicon nitride WRR are 9.6 cm and 5.37 cm, respectively. The measured free spectral range (FSR) of the silica WRR is 2.1 GHz. The measured free spectral range (FSR) of the silicon nitride WRR is 3.75 GHz. The RARs of the silica WRR and the silicon nitride WRR are 0.017 and 0.467, respectively. The demodulated output from LIA1 and LIA2, normally zero without rotation, will have two different nonzero values for an asymmetric resonance. As a result, the resonance asymmetry will cause bias error in the gyro's output.[6] It is necessary to carry out researches on the sources of resonance asymmetry and the influence of the resonance asymmetry. Finding out ways to reduce the resonance asymmetry and its influence are essential to achieving a high performance. To compare the influences of different sources on gyro output, the relevant parameters are set to be the same. The center frequency of FL is 193 THz. WRR length and effective refractive index are set to be 10 cm and 1.445, respectively. The PM1 and PM2 are driven by sinusoidal signals with frequencies of 1 MHz and 500 kHz, respectively. The width of resonance curve is set to be 20 MHz according to the fabrication level reported so far.[4] The power of the laser used in our RIOG is usually set to be tens of milliwatts to avoid being influenced by stimulated Brillouin scattering. Therefore, the nonlinear optical effects in the resonator are neglected.

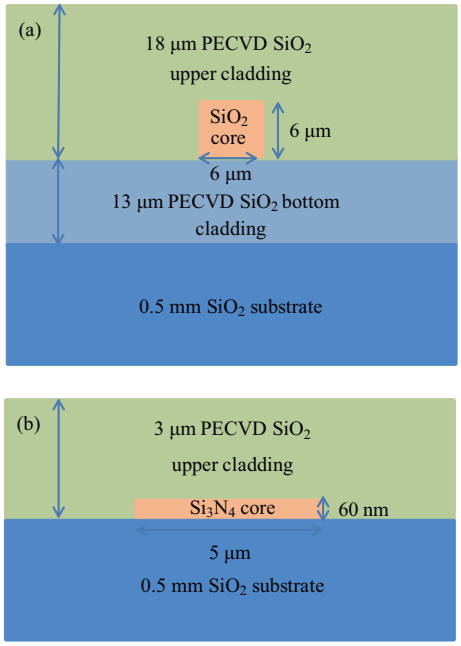


Fig. 3. (color online) Cross sections of (a) silica WRR and (b) silicon nitride.

3. Sources of resonance asymmetry

3.1. Polarization errors

A polarization-maintaining resonator supports two polarization states named eigenstates of polarization (ESOPs) that do not change their polarization states after circling one time in the resonator. The normalized received power of PD1 can be written as[12]

$$I_{\mathrm{PD1}} = \left\{(1-K)\left[1-\rho\Gamma(f)\right] + K\left[1-\rho\Gamma\left(f-\frac{\Delta\beta L}{2\pi\tau}\right)\right]\right\}\mathrm{e}^{-\alpha_c}I_0, \quad (2)$$

$$\Gamma(f) = \frac{\Delta f_{\mathrm{FWHM}}^2}{\Delta f_{\mathrm{FWHM}}^2 + 4(f-f_0)^2}, \quad (3)$$

$$\tau = nL/c, \quad (4)$$

where K is the excitation ratio of the unwanted ESOP, ρ is the depth of resonance curve, $\Delta\beta L$ is the phase difference between two ESOPs after one-round trip in the resonator, L and n are the length and the effective refractive index of the WRR, c is the speed of light, α_c is the loss of coupler, I_0 is the power of laser, Δf_{FWHM} is the full width at half maximum, and f_0 is the resonance frequency of WRR. The resonance curve will be asymmetric if the two resonance dips of the two ESOPs are close, which is shown in Fig. 4(a). Compared with Fig. 2(a), the resonance asymmetry of the silica WRR is probably caused by the polarization error. The phase difference between two ESOPs after one round trip in the resonator determines the asymmetric degree of the resonance curve. Figure 4(b) shows that the asymmetric degree reaches the highest points when the distance between two ESOPs is close to the half-width of resonance. According to the result of Fig. 4(b), the trend of gyro bias deviation is the same as that of the asymmetric degree. Figure 4(b) shows that the bias deviation from polarization error can be reduced by separating two dips of ESOPs.

3.2. Difference in loss between normal modes

In evanescent field directional couplers, there are generally two normal modes, i.e., a symmetric mode and an antisymmetric mode. Each of these normal modes may have different loss in traversing a coupler, which leads to a result that the phase difference between the through port and the cross port of a directional coupler deviates from $\pi/2$. According to the work by Youngquist *et al.*,[10] the resonance curve is plotted in Fig. 5(a). To plot the black curve, the loss for the antisymmetric mode is set to be $1-\rho_-^2 = 20$ percent and the loss for the symmetric mode is set to be $1-\rho_+^2 = 40$ percent with a waveguide ring transmission of $\rho_L^2 = 0.98$. The loss of the symmetric mode is set to be equal to the loss of antisymmetric mode for the red dash line. Figure 5(a) shows that the resonance curve will be symmetric when the losses for two normal modes are the same. Otherwise, the resonance curve will be asymmetric. Comparing with Fig. 2(b), the resonance asymmetry of the silicon nitride WRR is probably caused by this source. Assuming that the loss for the antisymmetric mode

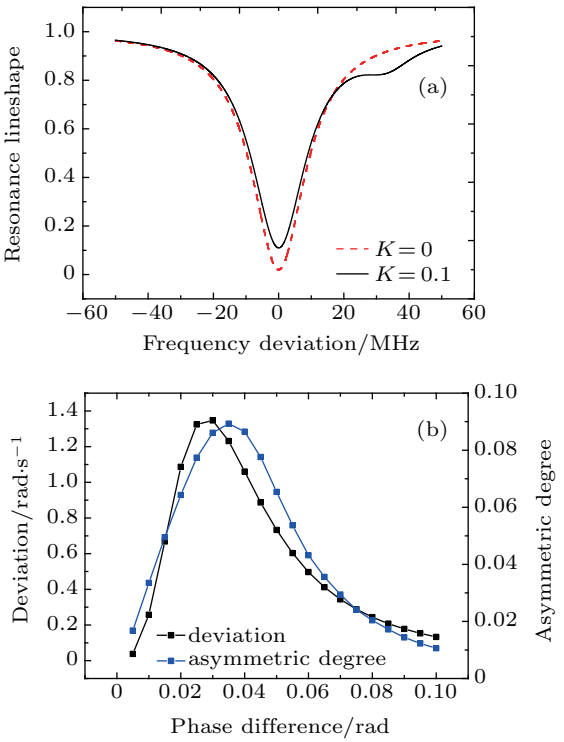


Fig. 4. (color online) (a) Calculated resonance curve when the excitation ratios of unwanted ESOP are 0 and 0.1; (b) relationships between gyro bias deviation and phase difference between two ESOPs, asymmetric degree, and phase difference of two ESOPs. The excitation ratio of unwanted ESOP is 0.1.

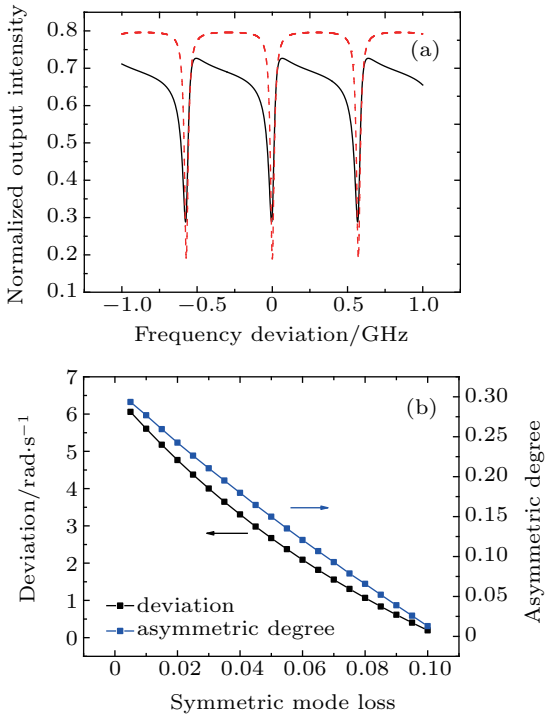


Fig. 5. (color online) Influence of normal modes loss. (a) Calculated resonance curves. Red curve: losses for two normal mode are different; black curve: losses for two normal mode are the same; (b) relationships between gyro's bias deviation and the loss for the symmetric mode while the loss for the antisymmetric mode is $1-\rho_-^2 = 10$ percent.

is $1-\rho_{-}^{2}=10$ percent, figure 5(b) is obtained while the loss for the symmetric mode varies. It shows that the asymmetric degree grows as the difference in loss between two normal modes increases. When the loss for the symmetric mode is $1-\rho_{+}^{2}=0$ percent, the RIOG bias error is calculated to be as high as 6.06 rad/s.

4. Discussion and solutions

From the above analysis, it can be concluded that the difference in normal mode loss can lead to a very strong asymmetry in the resonance curve. This asymmetry can be eliminated by using a different structure of resonator. There are two kinds of ring resonators, i.e., transmission resonators and reflector resonators, which are shown in Fig. 6. Considering the differential normal mode loss in the coupler, the resonance curve of a transmission resonator is more symmetric because all the output light beams have the same phase shift.[11] The modulation frequency is another factor that affects an RIOG bias error. The modulation frequency is always optimized to maximize the slope of the center part of the demodulated curve output from LIA, which is shown by blue dots in Fig. 7. However, an RIOG with modulation frequencies Δf_{21} and Δf_{22} has a bigger bias error than an RIOG with modulation frequencies Δf_{11} and Δf_{12}. Moreover, the small difference between modulation frequencies for LIA1 and LIA2 can reduce the bias error according to Fig. 7. Therefore, the difference between modulation frequencies for LIA1 and LIA2 is recommended to be not too big but also the backscattering noise can be reduced. The modulation frequencies for LIA1 and LIA2 are supposed to be optimized for each specific WRR.

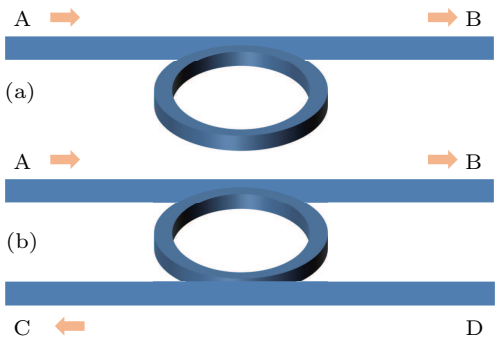


Fig. 6. (color online) Schematic diagrams of (a) reflector resonator, and (b) transmission resonator.

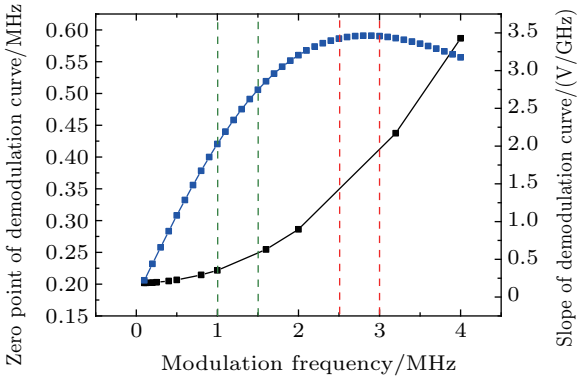


Fig. 7. (color online) Plots of slope of demodulated signal from LIA1 versus modulation frequency f_1 and zero points of the demodulated signal from LIA1 versus modulation frequency f_1. The resonance curve is the same as the black line in Fig. 3(a).

5. Conclusions

The resonance asymmetry phenomenon in a waveguide-type ring resonator optic gyro has been theoretically analyzed. The polarization error and difference in normal mode loss are discussed in detail. After analyzing their influences on gyro bias error, it is found that the bias error is not only determined by the RAR of the resonance curve but also varies with different source. A transmission resonator is recommended to obtain a better resonance curve based on the analysis. Proper modulation frequencies in clockwise (CW) and counterclockwise (CCW) directions can reduce an RIOG bias error.

References

[1] Jin J, Tian H T, Pan X and Song N F 2010 *Chin. Phys. B* **19** 030701
[2] Carroll R, Coccoli C, Cardarelli D and Coate G 1987 *Fiber Optic Gyros: 10th Anniversary Conference*, March 11, 1987, Cambridge, MA, USA, p. 169
[3] Ma H L, Jin Z H, Ding C and Wang Y L 2005 *Chin. J. Lasers* **32** 1330
[4] Zhang J J, Li H Z, Ma H L and Jin Z H 2017 *The 25th International Conference on Optical Fiber Sensors,* April 24–28, 2017, Jeju, Korea, p. 19
[5] Ciminelli C and Europ J 2014 *Opt. Soc. Rap. Public.* **9** 14013
[6] Chen Y, Ma H L and Jin Z H 2012 *Appl. Opt.* **51** 2373
[7] Zhang X L, Ma H L and Jin Z H 2006 *Appl. Opt.* **45** 7961
[8] Ma H L, He Z Y and Hotate K 2011 *J. Lightwave Technol.* **29** 85
[9] Ma H L, Chen Z, Yang Z H, Yu X H and Jin Z H 2012 *Appl. Opt.* **51** 6708
[10] Youngquist R, Stokes L and Shaw H 1983 *IEEE J. Quantum Electron.* **19** 1888
[11] Chang X, Ma H L and Jin Z H 2012 *Opt. Commun.* **285** 1134
[12] Iwatsuki K, Hotate K and Higashiguchi M 1986 *Appl. Opt.* **25** 2606